Science & Technology Development Journal 2023, 26(3):3017-3026
Open Access Full Text Article

A study on the optical properties of a novel flower-core photonic crystal fiber infiltrated with CCl_4

Nguyen Thi Thuy*

ABSTRACT

A novel design of a photonic crystal fiber with a flower core is proposed for the first time to optimize dispersion suitable for broadband supercontinuum generation. The numerical simulation of the propagation of light modes in optical fibers is computed by solving Maxwell's wave equations with the full-vector finite-difference eigenmode method. As a result, near-zero ultraflat all-normal and anomalous dispersion was achieved with fluctuations of $\pm$0.978 ps/nm.km in the 294 nm wavelength region and $\pm$1.168 ps/nm.km in the 432 nm wavelength region, respectively. The combination of CCl_4 infiltration into the hollow core and the air hole size heterogeneity in the cladding also enhances the nonlinear properties of the fibers. Effective mode areas less than 2 μm^2 at the pump wavelength can help the supercontinuum spectrum broaden further toward the red wavelength region. Three fibers with structural parameters Λ = 0.8 μm, d_1/Λ = 0.45, Λ = 0.9 μm, d_1/Λ = 0.5, Λ = 0.9 μm, and d_1/Λ = 0.45 are proposed for supercontinuum generation with low peak power due to nonlinear coefficients as high as hundreds of $W^{-1}.km^{-1}$. These new optical fibers could be highly efficient laser sources that replace traditional glass-core optical fibers.

Key words: Flower-core PCFs, CCl4 infiltration, ultraflat dispersion, high nonlinear coefficient, small effective mode area, low confinement loss, supercontinuum generation

INTRODUCTION

In recent years, hollow-core photonic crystal fibers (HPCFs) infiltrated with highly nonlinear liquids have been an excellent alternative to glass-core fibers, as they are particularly suitable for generating supercontinuum (SCG). This is because the nonlinear refractive index of these liquids is much higher when compared with fused silica, even up to 100 times greater than [1]. The flat dispersion with a low value, small effective mode area, high nonlinear coefficient, and low loss are all essential factors in improving SCG efficiency, which has been verified in HPCFs infiltrated with toluene (C_7H_8), chloroform ($CHCl_3$), benzene (C_6H_6), nitrobenzene ($C_6H_5NO_2$), and tetrachloroethylene (C_2Cl_4) [2–9]. The outstanding advantages of SCGs include the further spectral expansion in the near-infrared region, high-coherent spectrum, smoothness, low noise, and flat-top, making them have a wide range of applications in the fields of optical communication, fiber optic sensing, optical coherence tomography, optical metrology and spectroscopy [10–14].

The continuous development of fiber optic technology and the introduction of new materials are endless sources of inspiration for researchers in the design of novel optical fibers. Accordingly, the structural parameters of HPCFs are also always targeted to drastically change the optical properties of the fibers, which is beneficial for different applications. Many previous publications have mentioned different fiber designs, such as substrates or composites for whole or part of the optical fiber [15,16], cross-sections with different geometries [17], changes in the core diameter, air hole diameter, and the distance between two adjacent air holes [3,4,7,9]. This study is also one such motivation, and we propose flower-core HPCFs filled with carbon tetrachloride (CCl_4) as a novel fiber for potential nonlinear applications. CCl_4 is a very interesting nonlinear liquid, and its nonlinear refractive index is 5 times higher than that of silica [1], which will create a large difference in the refractive index between the cladding and the core, causing the light modes to be confined better in the core. Moreover, its low toxicity (compared to liquids such as carbon disulfide, nitrobenzene, and toluene [18]) ensures safety in fiber fabrication. In particular, CCl_4 and silica have similar linear refractive indices [19], which will enhance the coupling efficiency in all-fiber pump laser systems.

Several previous papers have demonstrated the ability to achieve a broad SCG spectrum using silica-based HPCFs infiltrated with CCl_4. Hexagonal, circular, and square lattices are quite commonly modeled. A flat all-normal dispersion with a value of −4.37 ps/nm.km at a pump wavelength of 1.55 μm was used

University of Education, Hue University, 34 Le Loi, Hue City, Vietnam

Correspondence

Nguyen Thi Thuy, University of Education, Hue University, 34 Le Loi, Hue City, Vietnam

Email: nguyenthithuy@dhsphue.edu.vn; ntthuy@hueuni.edu.vn

History
- Received: 2023-07-27
- Accepted: 2023-09-15
- Published Online: 2023-09-30

DOI :
https://doi.org/10.32508/stdj.v26i3.4136

Cite this article : Thuy N T. **A study on the optical properties of a novel flower-core photonic crystal fiber infiltrated with CCl_4**. *Sci. Tech. Dev. J.* 2023; 26(3):3017-3026.

to emit broadband SCG[20]. Experimentally, article[21] showed that the ability to obtain all-normal dispersion varies from −150 to 0 ps/nm.km in the wide wavelength region. The effective mode area of 42.2 μm^2 and the nonlinear coefficient of 221 $W^{-1}.km^{-1}$ contributed to the spectral expansion spanning from 850 to 1250 nm. The flat dispersion and characteristic quantities with values suitable for SCG spectral expansion are also reported experimentally in paper[22]. However, the values of the quantities characteristic in these reports have not been optimized simultaneously. The nonlinear coefficients of HPCFs are still low, and the effective mode area is still large, which causes the SCG spectrum to not broaden as expected[20]. To eliminate such limitations, a different approach in HPCF design with differences in the air hole size in the cladding was presented[23,24]. Two optimized HPCFs with flat all-normal and anomalous dispersion and low values of −9.376 and 1.015 ps/nm.km enabled SCG spectra as broad as 768 and 1751.1 nm with flat-top[23]. Similarly, work[24] also demonstrates the ability to achieve HPCFs with low dispersion, small effective mode area, and low confinement loss.

Our new design combines two methods. First, the hollow flower-core infiltrate to CCl_4 will create a large difference between the refractive index of the core and the cladding. Second, the air hole in the first ring is smaller than the others, making it easy to control dispersion and loss. Thus, we obtained ultraflat dispersions with variable values of ±0.978 ps/nm.km and ±1.168 ps/nm.km in the wavelength regions of 294 nm and 432 nm, respectively, for optimal optical fibers. In addition, the nonlinear properties of the proposed fibers are also analyzed in detail to guide SCGs with low peak power.

MATERIALS-METHODS

The idea of designing these HPCFs is based on works[3,6,24] and[25], which emphasize the role of the size of the air holes in the cladding. The dispersion properties can be easily controlled if the air hole in the first ring is not the same as the others. The loss in the fundamental mode or higher-order modes can be improved by the influence of subsequent rings. Therefore, the air holes in the first ring are designed with diameter d_1, which is smaller than d_2 (d_2 is the diameter of the other holes). The distance between two adjacent air holes is pitch Λ , and the hollow core has diameter D_c. The design parameters are shown in Table 1. Figure 1a shows the cross-sectional view of the HPCF with a flower-shaped hollow core. The lattice has a regular hexagonal structure with a flower-shaped core being the largest air hole in the center filled with CCl_4. The first ring in the cladding has six small air holes evenly spaced around the core. The air holes in the other seven rings are larger in size and are designed parallel to the axis of the core. Figure 1b confirms the well-confined light modes in the core of the HPCF with Λ = 0.8 μm and d_1/Λ = 0.45.

Maxwell's wave equations are used to calculate the propagation coefficients and modes of electromagnetic fields in HPCFs using Lumerical Mode Solutions (LMS) software. The boundary conditions are perfectly matched layers that are subdivided to reduce the loss to the smallest possible value. The cross-section of HPCFs is approximately a few micro μm^2, which is divided into hundreds of thousands of rectangles to reduce the meshing error of the simulations. The optical properties of the HPCFs are simulated through the LMS with the full-vector finite-difference eigenmode (FDE) method. Fused silica and CCl_4 were established and entered into the LMS by declaring the Sellmeier and Cauchy coefficients from **Equations** (**1**) and (**2**)[26,27]. It is not too difficult to experimentally fabricate CCl_4-infiltrated HPCFs. The stack-and-draw method is commonly used for spinning, while the fluids are introduced into the core via a pump system with a laser writing technique or a thermal fusion splicer[22,28]. Figure 1c shows that the linear refractive index of fused silica and CCl_4 both decrease with wavelength and that the difference in the index of the two materials is not too large.

$$n^2_{CCl_4}(\lambda) = 2.085608282 + 0.0053373\lambda^2 + 0.012201206\lambda^{-2} + 0.000056451\lambda^{-4} + 0.000048106\lambda^{-6}, \quad (1)$$

$$n^2_{SiO_2}(\lambda) = 1 + \frac{0.6961663\lambda^2}{\lambda^2 - 0.0684043^2} + \frac{0.4079426\lambda^2}{\lambda^2 - 0.1162414^2} + \frac{0.8974794\lambda^2}{\lambda^2 - 9.896161^2}, \quad (2)$$

where λ is the wavelength and $n(\lambda)$ is the linear refractive index of the materials.

The dispersion is the fast or slow propagation over time of different frequency components of a light pulse in a nonlinear optical medium such as an optical fiber. This is the result of the interaction of light with electrons in the medium. It is an important parameter that governs the efficiency of the SCG generation process. The flatness over a wide wavelength range, low dispersion gradient, small dispersion value, all-normal or anomalous nature of dispersion, and shift of zero dispersion wavelength (ZDW) have always been the first goals of optical fiber designs in theoretical simulations as well as experiments. The dispersion

Table 1: The structural parameters of HPCFs with CCl_4 infiltration

d1/Λ	Λ = 0.8 μm			Λ = 1.5 μm		
	d1 μm)	d2 μm)	Dc μm)	d1 (μm)	d2 (μm)	Dc μm)
0.3	0.24	0.76	1.48	0.45	1.43	2.78
0.35	0.28	0.76	1.45	0.53	1.43	2.71
0.45	0.36	0.76	1.37	0.68	1.43	2.56
0.5	0.40	0.76	1.32	0.75	1.43	2.48
0.55	0.44	0.76	1.27	0.83	1.43	2.38
0.6	0.48	0.76	1.22	0.90	1.43	2.28
0.65	0.52	0.76	1.16	0.98	1.43	2.17
	Λ = 0.9 μm			Λ = 2.0 μm		
0.3	0.27	0.86	1.67	0.60	1.90	3.70
0.35	0.32	0.86	1.63	0.70	1.90	3.62
0.45	0.41	0.86	1.54	0.90	1.90	3.42
0.5	0.45	0.86	1.49	1.00	1.90	3.30
0.55	0.50	0.86	1.43	1.10	1.90	3.18
0.6	0.54	0.86	1.37	1.20	1.90	3.04
0.65	0.59	0.86	1.30	1.30	1.90	2.90

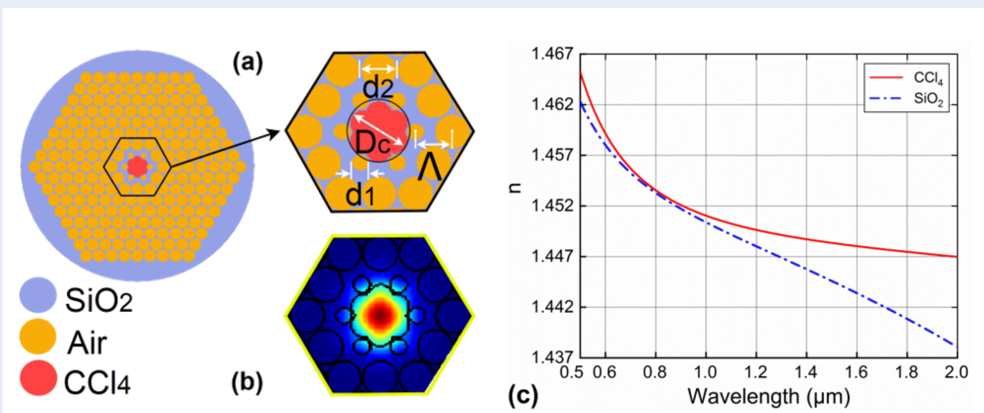

Figure 1: The cross-sectional view of the HPCF, flower-shaped hollow core in the center, surrounded by six air holes of smaller size, the remaining air holes are arranged regularly into 7 rings in the cladding (a). The linear refractive index of fused silica and CCl_4 varies with wavelength (b).

is calculated through the real part of the effective refractive index (Re[n_{eff}]), the wavelength (λ), and the speed of light in a vacuum (c) according to the following formula[29]:

$$D_c = -\frac{\lambda}{c}\frac{dRe\left[n_{eff}\right]}{d\lambda^2}. \quad (3)$$

The nonlinearity of optical fibers is characterized by a number of characteristic quantities, such as the nonlinear coefficient (γ), effective mode area (A_{eff}), and confinement loss (L_c). They are computed through the equations below[29]. The properties of the SCG spectrum are strongly influenced by these quantities, but it is difficult to optimize them simultaneously. The more relevant values are, the more beneficial the SCG.

$$\gamma(\lambda) = 2\pi\frac{n_2}{\lambda A_{eff}}, \quad (4)$$

where n_2 is the nonlinear refractive index of fused silica.

$$A_{eff} = \frac{\left(\int_{-\infty}^{\infty}\int_{-\infty}^{\infty}|E|^2dxdy\right)^2}{\int_{-\infty}^{\infty}\int_{-\infty}^{\infty}|E|^4dxdy} \quad (5)$$

$$L_c = 8.686\frac{2\pi}{\lambda}Im\left[n_{eff}\right], \quad (6)$$

where Im [n_{eff}] is the imaginary part of the effective refractive index.

RESULTS

The diversity in dispersion is the expected result for CCl_4-infiltrated flower-core HPCFs. All-normal and anomalous dispersions with one or more ZDWs are found with different fiber structures, demonstrating that the structural parameters (d_1/Λ and Λ) strongly influence the dispersion properties (Figure 2). When Λ = 0.8 μm, there are three anomalous dispersion curves with small d_1/Λ (d_1/Λ = 0.3, 0.35, 0.4). They intersect the zero dispersion line at a point corresponding to the ZDW. Moreover, these ZDWs shift toward a longer wavelength range as d_1/Λ increases. Increasing d_1/Λ further, the dispersion curves are increasingly compressed down from the zero dispersion line, becoming all-normal dispersion properties. In particular, we obtained a near-zero ultraflat all-normal dispersion curve with the structure d_1/Λ = 0.45, the range of variation $\pm$0.978 ps/nm.km spanning from the wavelength 1379 nm to 1673 nm. Increasing Λ to 0.9 μm, the dispersion curves tend to shift above the zero dispersion line, all of which are anomalous dispersion curves with one ZDW ($d_1/\Lambda \leq$ 0.45) and two ZDWs ($d_1/\Lambda \geq$ 0.5). The HPCF with structure Λ = 0.9 μm and d_1/Λ = 0.5 is the flattest anomalous dispersion curve, and the dispersion value varies $\pm$1.168 ps/nm.km in the wavelength range of 1420−1852 nm. Continuing to increase Λ (Λ = 1.5 and 2.0 μm), the all-normal dispersion curves no longer appear. Instead, all curves are anomalous dispersions with ZDW shifting to the short wavelength region when the value of d_1/Λ rises. Table 2 illustrates the values of ZDW according to the variation in d_1/Λ. The shift of ZDW toward long wavelengths is very significant in selecting suitable pump wavelengths for SCG generation. HPCFs with ZDW closer to 1.55 μm are beneficial factors because this is the wavelength of commercially available lasers. The dispersion values are also calculated at a wavelength of 1.55 μm, as verified in Table 3.

Based on preliminary results on dispersion properties, we proposed three HPCFs with suitable dispersion characteristics for detailed analysis and orientation for SCG application (Figure 3a). They are #F_1 (Λ = 0.8 μm, d_1/Λ = 0.45), #F_2 (Λ = 0.9 μm, d_1/Λ = 0.5), and #F_3 (Λ = 0.9 μm, d_1/Λ = 0.45). The confinement loss, effective mode area, and nonlinear coefficient are calculated with the results shown in Figure 3b-d. The structural parameters and the values of the characteristic quantities at the pumping wavelength of the three optimal wavelengths are presented in Table 4. The way to select the appropriate pump wavelength for SCGs using the three proposed structures must be based on the following: First, the value of the dispersion, which is sufficiently small or close to the ZDW for anomalous dispersions, or a value close to the local maximum of the all-normal dispersion curve. Second, match the pump wavelengths of commercial laser sources. Therefore, the selected pump wavelengths are 1.55 μm for the #F_1 fibers and 1.064 μm for the #F_2 and #F_3 fibers.

DISCUSSION

The diversity in dispersion results of CCl_4-infiltrated HPCFs opens up many opportunities for SCG applications for both anomalous and all-normal dispersion. We obtained two near-zero ultraflat dispersions for both all-normal (Λ = 0.8 μm, d_1/Λ = 0.45) and anomalous (Λ = 0.9 μm, d_1/Λ = 0.45) (Figure 2a, b) with low dispersion values. This is significant because previous publications on CCl_4-infiltrated HPCFs have yet to find such dispersions, although every design effort has been performed to control dispersion[20–24,30].

The different dispersion properties will be responsible for different SCG spectral characteristics. To obtain a wide SCG spectrum, low noise, high coherence, and flat-top, it is common to pump the fiber in the all-normal dispersion regime. Then, the soliton dynamics, especially the separation of higher-order solitons

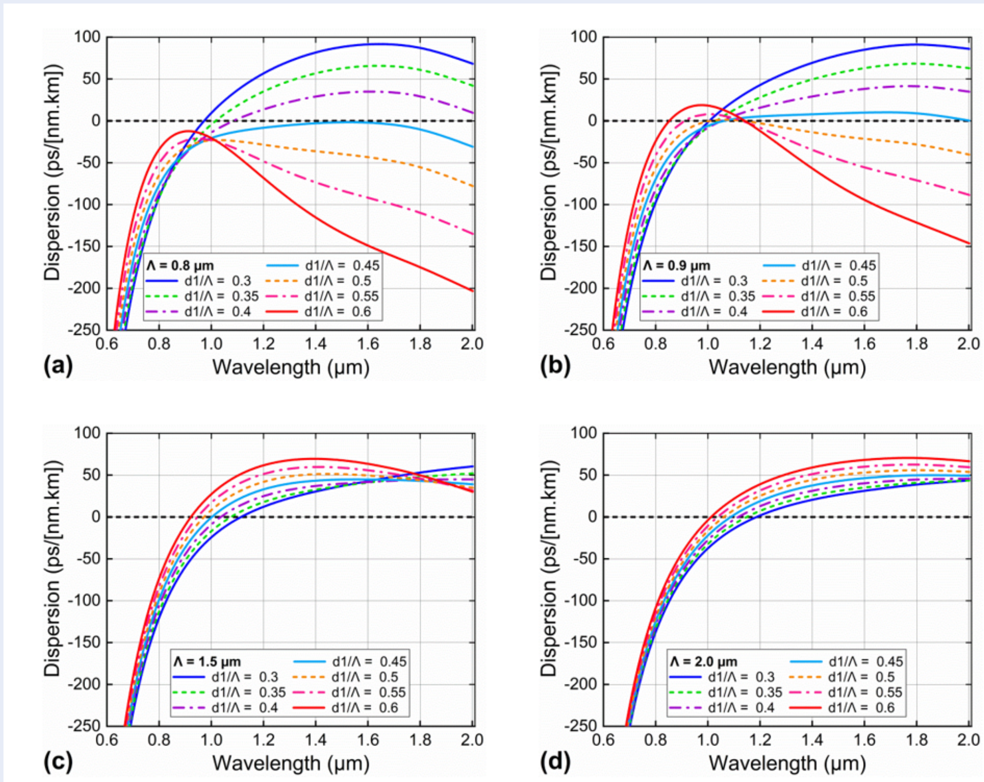

Figure 2: The dispersion against wavelength with HPCFs of different structure parameters, the filling factor d_1/Λ varies from 0.3 to 0.6, with $\Lambda = 0.8\ \mu$m (a), 0.9 μm (b), 1.5 μm (c), and 2.0 μm (d)

Table 2: The ZDW values of infiltrated-CCl_4 HPCFs with variations in Λ and d_1/Λ

	$\Lambda = 0.8\ \mu$m	$\Lambda = 0.9\ \mu$m		$\Lambda = 1.0\ \mu$m	$\Lambda = 1.5\ \mu$m
d_1/Λ	ZDW_{s1}	ZDW_{s1}	ZDW_{s2}	ZDW_{s1}	ZDW_{s1}
0.3	0.972	1.005		1.113	1.185
0.35	1.016	1.031		1.074	1.147
0.4	1.083	1.05		1.034	1.116
0.45	D < 0	1.062		1.001	1.086
0.5	D < 0	1.006	1.137	0.971	1.06
0.55	D < 0	0.91	1.133	0.946	1.035
0.6	D < 0	0.85	1.142	0.921	1.012

from the elementary solitons, which are responsible for the noise of the spectrum, are suppressed [31]. In this case, four-wave mixing and self-phase modulation followed by optical wave breaking are the main mechanisms that strongly influence spectral expansion. In contrast, very large SCG bandwidths, even several octaves, can be achieved thanks to the dominance of soliton-related effects such as soliton fission, soliton self-frequency shift, and blueshifted dispersive waves[31], but the spectrum is very noisy and has low coherence.

#F_1 fiber with an all-normal dispersion profile, dispersion variation as small as ± 0.978 ps/nm.km in the 294 nm wavelength range, and dispersion value of -1.453 ps/nm.km is expected to generate a smooth, noiseless, broad spectrum SCG at a 1.55 μm pump wavelength. Such SCGs will have high potential in applications such as optical coherence tomography,

Table 3: Dispersion values at 1.55 μm of infiltrated CCl_4 HPCFs with variations in Λ and d_1/Λ

d_1/Λ	D (ps/nm.km)			
	Λ = 0.8 μm	Λ = 0.9 μm	Λ = 1.0 μm	Λ = 1.5 μm
0.3	90.691	82.299	40.084	29.149
0.35	64.936	60.609	39.292	33.447
0.4	34.861	36.562	41.034	38.812
0.45	−1.453	9.496	44.973	45.024
0.5	−41.27	−19.829	50.746	51.789
0.55	−87.731	-51.2	57.746	58.828
0.6	−141.968	−86.376	66.199	66.914

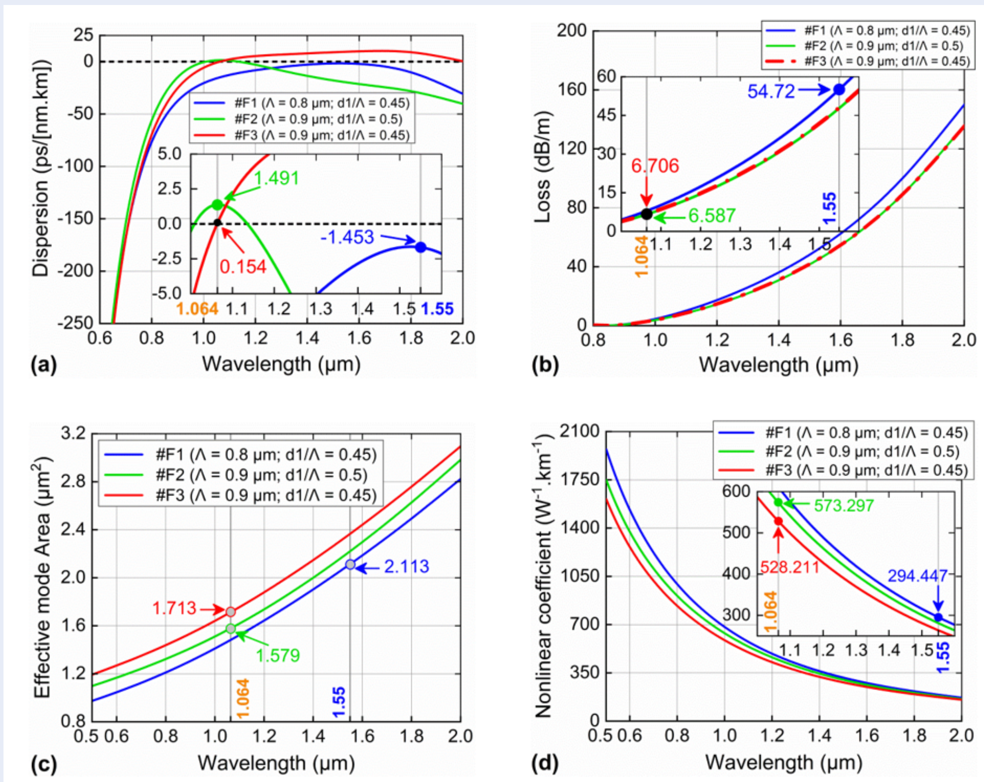

Figure 3: The wavelength-dependent characteristic quantities of the three proposed HPCFs, #F_1 (Λ = 0.8 μm, d_1/Λ = 0.45), #F_2 (Λ = 0.9 μm, d_1/Λ = 0.5), and #F_3 (Λ = 0.9 μm, d_1/Λ = 0.45). (a) The dispersion versus wavelength curve, the right inset illustrates the dispersion values at the pump wavelength.
(b) The confinement loss is a function of wavelength, the left inset shows the L_c values at the pump wavelength.
(c) The effective mode area increases with wavelength, the A_{eff} values at the pump wavelength are also testified on the graphs.
(d) The nonlinear coefficient is wavelength dependent, the right inset displays the γ values at the pump wavelength.

Table 4: The structural parameters and the values of the characteristic quantities at the pump wavelength of the three proposed HPCFs

#	D_c	Λ	d_1/Λ	Pump wave-length	Re[n_{eff}]	D	L_c	A_{eff}	γ
	(μm)	(μm)		(μm)	(real)	(ps/nm.km)	(dB/m)	(μm^2)	($W^{-1}.km^{-1}$)
#F1	1.366	0.8	0.45	1.55	1.326	−1.453	54.72	2.113	294.447
#F2	1.485	0.9	0.5	1.064	1.383	1.491	6.587	1.579	573.297
#F3	1.537	0.9	0.45	1.064	1.388	0.154	6.706	1.713	528.211

spectroscopy and metrology[32]. The #F_2 fiber has anomalous dispersion with two very close ZDWs of 1.006 μm and 1.137 μm (Table 2). Although a pump wavelength of 1.064 μm is chosen in the anomalous dispersion region and a small dispersion value of 1.491 ps/nm.km, the obtained SCG spectra would be in stark contrast to standard photonic crystal fibers that have anomalous dispersion with only one ZDW or two ZDWs far apart[15,33]. In such fibers, the Four-Wave Mixing effect becomes a major factor that makes the SCG spectrum broader while the soliton dynamics are captured and play a barely significant role in the formation of the supercontinuum[15]. The spectral characteristics are similar to those of SCG using fibers with all-normal dispersion. The #F_3 fiber has a near-zero ultraflat anomalous dispersion profile with one ZDW, and the pumping wavelength is 1.064 μm larger than that of ZDW (1.062 μm), which will enable a very broad SCG spectrum, broader than the two fibers #F_1 and #F_2, but the spectrum will be much noisier. Of the three proposed fibers, the dispersion value at the pump wavelength of the #F_3 fiber is 0.154 ps/nm.km, which is nearly 10 times smaller than that of #F_1 and #F_2 (Table 4). In addition, the dispersion values obtained for these three optimal fibers are hundreds of times smaller than those in work[21]. Compared with paper[20], the #F_1 and #F_2 fibers have an approximately three times smaller dispersion at the pump wavelength. The small dispersion value of the #F_3 fiber at the pump wavelength will be a good condition to broaden the SCG spectrum more than previously published. This value is between 6.5 and 60 times smaller than the optimal optical fibers verified in work[24].

The confinement loss is the loss that should be minimized during the simulation of HPCFs to ensure that the power of the propagation is not reduced. It is a loss that is incurred due to leakage of modes from the core to the cladding or between the air holes or due to the imperfect structure of the optical fibers. Therefore, the confinement loss is affected by the wavelength, pitch Λ, number of air hole rings, and air hole size. Figure 3b shows that the low-frequency components (long wavelength) leak more so that L_c increases in this wavelength region. In the short wavelength region, the L_c of the three fibers is quite similar ($\lambda < 1.0$ μm), but the difference in values is larger in the longer wavelength region. The #F_1 fiber has a larger L_c in the wavelength range $\lambda > 1.0$ μm, while the L_c of the other two fibers is almost the same. For the three proposed fibers, the L_c value at the pump wavelengths is quite suitable for SCG application. Fiber #F_1 has the highest L_c of 54.72 dB/m compared to the other two fibers, and #F_2 and #F_3 have L_c values of 6.587 and 6.706 dB/m, respectively (Table 4). Thus, the SCG progress using the #F_1 fiber will probably be more limited in extending the spectrum toward the red wavelength region compared to #F_2 and #F_3. In comparison with #SF_1, #SF_2, and #CF_2 fibers with square and circular lattices in publication[24], the L_c values of #F_2 and #F_3 fibers are approximately 2.5 to 4 times smaller.

The effective mode area is related to the energy density of the light mode per unit length of the fiber and its maximum energy density. A_{eff} increases as the wavelength increases, as shown in Figure 3c. Longer wavelengths are more difficult to confine to the core than shorter wavelength components. In addition, the core size is also a parameter that affects the value of A_{eff}. Smaller cores often exhibit better light restriction in the core, although being too small makes fiber fabrication more difficult. The #F_1 fiber has the smallest A_{eff} in the investigated wavelength region due to having the smallest core (D_c = 1.366 μm) (Table 4). This leads to its highest nonlinear coefficient in the entire wavelength range (Figure 3d) because the two quantities are inversely proportional to each other. However, at a pump wavelength of 1.55 μm, this fiber has γ = 294.447 $W^{-1}.km^{-1}$, which is less high than that of fibers #F_2 and #F_3 (573.297 and 528.211 $W^{-1}.km^{-1}$) because their γ is chosen at the pump wavelength of 1.064 μm. The high value of γ contributes to the broadened SCG spectrum with low input pulse peak

Table 5: The characteristic quantities at the pump wavelength of three proposed HPCFs in comparison with some previous work on liquid-filled HPCFs

#	Refs.	Pump wavelength (μm)	D (ps/nm.km)	L_c (dB/m)	Aeff (μm^2)	γ ($W^{-1}.km^{-1}$)
#F1	This work	1.55	−1.453	54.72	2.113	294.447
#F2	This work	1.064	1.491	6.587	1.579	573.297
#F3	This work	1.064	0.154	6.706	1.713	528.211
CCl_4, #F_1	20	1.35	12	–	–	–
CCl_4, #F_2		1.55	−4.37	–	10.58	–
CCl_4, #SF_1	24	1.095	−6.577	17.833	2.186	404.924
CCl_4, #SF_2		1.30	1.331	28.186	10.479	84.493
CCl_4, #CF_1		0.98	−9.376	4.545	1.513	585.025
CCl_4, #CF_2		1.30	1.015	19.406	8.735	101.371
C_7H_8, #F_1	3	1.55	0.489	–	2.527	2699.919
C_7H_8, #F_2		1.55	–1.534	–	2.632	2592.282
$CHCl_3$, #F_1	4	0.945	−1.629	2.477	1.43	763.313
$CHCl_3$, #F_2		1.40	2.619	39.628	11.524	63.913
C_2Cl_4, #F_1	8	1.56	−15.0	4.0	433.2	156.9
C_2Cl_4, #F_2		1.56	3.20	4.2	16.67	40.79
C_2Cl_4, #F_3		1.03	−4.85	5.3	359.1	189.3

power (the femtosecond duration and nano Joule energy)[3,4,8,9]. The proposed three fibers also provide smaller A_{eff} and higher γ values than some of the optical fibers in previous publications of CCl_4-filled HPCF[20–24]. Even when compared with HPCFs infiltrated with other nonlinear liquids, we obtain a better characteristic quantity at the pump wavelength. The results of this comparison are presented in Table 5.

CONCLUSIONS

We designed a novel structure of hexagonal lattice photonic crystal fiber with a flower-shaped hollow core filled with CCl_4. The dispersion and nonlinear properties of the fiber are investigated by numerical simulation based on solving Maxwell's wave equations with the FDE method. Some of the outstanding results of this work are as follows:

First, a near-zero ultraflat all-normal dispersion with small fluctuations of ± 0.978 ps/nm.km, covering the wavelength region $1379-1673$ nm, is achieved with $\Lambda = 0.8$ μm and $d_1/\Lambda = 0.45$.

Second, the structure $\Lambda = 0.9$ μm, $d_1/\Lambda = 0.45$ exhibits near-zero ultraflat anomalous dispersion with a variation value of ± 1.168 ps/nm.km, spanning from 1420 to 1852 nm.

Third, we propose three structures, #F_1, #F_2, and #F_3, with flat dispersion and small values of -1.453, 1.491, and 0.154 ps/nm.km at wavelengths of 1.55, 1.064, and 1.064 μm, respectively. In comparison with previous publications, we confirm that suitable characteristic quantities of these fibers, such as the small effective mode area, high nonlinear coefficient, and low confinement loss, are favorable conditions to generate broadband supercontinuum with low peak power.

We also analyzed the dispersion and nonlinear properties of the proposed three fibers in detail to guide the appropriate application of supercontinuum generation for each fiber type. The proposed fibers can be low peak power supercontinuum generation sources replacing traditional glass core fibers.

ABBREVIATIONS

SCG: Supercontinuum generation

HPCFs: Hollow-core Photonic Crystal Fibers

ZDW: zero dispersion wavelength

LMS: Lumerical Mode Solutions

FDE: Finite Difference Eigenmode

COMPETING INTERESTS

The authors declare that they have no conflicts of interest.

AUTHORS' CONTRIBUTIONS

Thuy Nguyen Thi: Designing and simulating the PCF structures, Data analysis, Data processing, Plotting graph, Methodology, Writing manuscript, Answering the reviewer's questions.

ACKNOWLEDGEMENTS

None.

REFERENCES

1. Ho P and Alfano R. Optical Kerr effect in liquids. Physical Review A. 1979;20:2170-2187;Available from: https://doi.org/10.1103/PhysRevA.20.2170.
2. Thi TN, Trong DH, Tran BTL, Van TD, Van LC. Optimization of optical properties of toluene-core photonic crystal fibers with circle lattice for supercontinuum generation. Journal of Optics. 2022;51:678-688;Available from: https://doi.org/10.1007/s12596-021-00802-y.
3. Thi TN, Trong DH, Van LC. Supercontinuum generation in ultraflattened near-zero dispersion pcf with C7H8 infiltration. Optical and Quantum Electronic. 2023;55:93;Available from: https://doi.org/10.1007/s11082-022-04351-x.
4. Thi TN, Van LC. Supercontinuum spectra above 2700 nm in circular lattice photonic crystal fiber infiltrated chloroform with the low peak power. Journal of Computational Electronics. 2023;Available from: https://doi.org/10.1007/s10825-023-02078-w.
5. Van LC, Hoang VT, Long VC, Borzycki K, Xuan KD, Quoc VT, Trippenbach M, Buczyński R, Pniewski J. Optimization of optical properties of photonic crystal fibers infiltrated with chloroform for supercontinuum generation. Laser Physics. 2019;29(7):075107-9;Available from: https://doi.org/10.1088/1555-6611/ab2115.
6. Van LC, Hoang VT, Long VC, Borzycki K, Xuan KD, Quoc VT, Trippenbach M, Buczyński R, Pniewski J. Supercontinuum generation in benzene-filled hollow-core fibers. Optical Engineering. 2021;60(11):116109;Available from: http://doi.org/10.1117/1.OE.60.11.116109.
7. Van LC, Tran BTL, Thi TN, Trong DH, Van TD, Mai TD, Ngoc HT, Doan TT, Quoc KD. Comparison of supercontinuum generation spectral intensity in benzene-core pcfs with diferent types of lattices in the claddings. Optical and Quantum Electronics. 2022;54:840;Available from: https://doi.org/10.1007/s11082-022-04218-1.
8. Hieu VL, Van TH, Hue TN, Van CL, Buczynski R, Kasztelanic R. Supercontinuum generation in photonic crystal fibers infiltrated with tetrachloroethylene. Optical and Quantum Electronics. 2021;53:187;Available from: https://doi.org/10.1007/s11082-021-02820-3.
9. Van LC, Thi TN, Trong DH, Tran BTL, Minh NVT, Van TD, Canh TL, Dinh QH, Quoc KD. Comparison of supercontinuum spectrum generating by hollow core PCFs filled with nitrobenzene with different lattice types. Optical and Quantum Electronics. 2022;54:300;Available from: https://doi.org/10.1007/s11082-022-03667-y.
10. Chemnitz M, Gebhardt M, Gaida C, Stutzki F, Kobelke J, Limpert J. Hybrid soliton dynamics in liquid-core fbres. Nature Communications. 2017;8:42;PMID: 28663548. Available from: https://doi.org/10.1038/s41467-017-00033-5.
11. Madani SA, Bahrami M, Rostami A. Modulation instability and highly sensitive optical fiber biosensor. Optics Continuum. 2022;1(4):816-825;Available from: https://doi.org/10.1364/OPTCON.456317.
12. Lühder TAK, Chemnitz M, Schneidewind H, Schartner EP, Ebendorff-Heidepriem H, Schmidt MA. Tailored multicolor dispersive wave formation in quasiphase-matched exposed core fibers. Advanced Science. 2022;9(8):2103864;Available from: https://doi.org/10.1002/advs.202103864.
13. Jia J, Kang Z, Huang Q, He S. Mid-infrared highly efficient, broadband, and flattened dispersive wave generation via dual-coupled thin-film lithium-niobate-on-insulator waveguide. Applied Sciences. 2022;12(18):9130;Available from: https://doi.org/10.3390/app12189130.
14. Cui Q, Chen Z, Liu Q, Zhang Z, Luo Q, Fu L. Visible continuum pulses based on enhanced dispersive wave generation for endogenous fluorescence imaging. Biomedical Optics Express. 2017;8(9):4026–4036;Available from: https://doi.org/10.1364/BOE.8.004026.
15. Ghanbari A, Kashaninia A, Sadr A, Saghaei H. Supercontinuum generation for optical coherence tomography using magnesium fluoride photonic crystal fiber. Optik. 2017;140:545–554;Available from: https://doi.org/10.1016/j.ijleo.2017.04.099.
16. Trong DH, Tran BTL, Dinh LV, Van LC, Thi TN. Optimization of the optical properties of circular lattice As2Se3 photonic crystal fibers over a wide range of wavelengths. VNUHCM Journal of Science and Technology Development. 2022;25(4):2581–2593;Available from: https://doi.org/10.32508/stdj.v25i4.3989.
17. Alam MdZ, Tahmid MdI, Mouna ST, Islam MdA, Alam MS. Design of a novel star type photonic crystal fiber for mid-infrared supercontinuum generation. Optics Communications. 2021;500:127322;Available from: https://doi.org/10.1016/j.optcom.2021.127322.
18. Challenor J. Toxicology of solvents. Rapra Technology Ltd. ISBN: 1-85957-296-0. 2002;Available from: https://doi/10.1093/occmed/52.6.363-a.
19. Meister J, Franzen R, Eyrich G, Bongartz J, Gutknecht N, Hering P. First clinical application of a liquid-corelight guide connected to an Er: YAG laser for oral treatment of leukoplakia, Laser Medical Science. 2010;25(5):669-673;Available from: https://doi.org/10.1007/s10103-010-0782-0.
20. Dinh QH, Pniewski J, Van HL, Ramaniuk A, Long VC, Borzycki K, Xuan KD, Klimczak M, Buczyński R. Optimization of optical properties of photonic crystal fibers infiltrated with carbon tetrachloride for supercontinuum generation with subnanojoule femtosecond pulses. Applied Optics. 2018;57(14):3738–3746;Available from: https://doi.org/10.1364/AO.57.003738.
21. Hoang VT, Kasztelanic R, Filipkowski A, Stępniewski G, Pysz D, Klimczak M, Ertman S, Long VC, Woliński TR, Trippenbach M, Xuan KD, Śmietana M, Buczyński R. Supercontinuum generation in an all-normal dispersion large core photonic crystal fiber infiltrated with carbon tetrachloride. Optical Materials Express. 2019;9(5):2264–2278;Available from: https://doi.org/10.1364/OME.9.002264.
22. Hoang VT, Kasztelanic R, Stępniewski G, Xuan KD, Long VC, Trippenbach M, Klimczak M, Buczyński R, Pniewski J. Femtosecond supercontinuum generation approximately 1560nm in hollow-core photonic crystal fibers filled with carbon tetrachloride. Applied Optics. 2020;59(12):3720–3725;Available from: https://doi.org/10.1364/AO.385003.
23. TN Thi, DH Trong, BTL Tran, LC Van. Flat-top and broadband supercontinuum generation in CCl4-filled circular photonic crystal fiber. Journal of Nonlinear Optical Physics & Materials. 2023:2350042–19;Available from: https://doi.org/10.1142/S021886352350042X.
24. TN Thi, DH Trong, LC Van. Comparison of supercontinuum spectral widths in CCl4-core PCF with square and circular lattices in the claddings. Laser Physics. 2023;33(5):055102–13;Available from: https://doi.org/10.1088/1555-6611/acc240.

25. Saitoh K, Koshiba M, Hasegawa T, Sasaoka E. Chromatic dispersion control in photonic crystal fibers: application to ultraflattened dispersion. Optics Express. 2003;11(8):843-852;PMID: 19461798. Available from: https://doi.org/10.1364/OE.11.000843.
26. Moutzouris K, Papamichael M, Betsis SC, Stavrakas I, Hloupis G, Triantis D. Refractive, dispersive and thermo-optic properties of twelve organic solvents in the visible and near-infrared. Applied Physics B. 2013;116(3):617-622;Available from: https://doi.org/10.1007/s00340-013-5744-3.
27. Tan CZ. Determination of refractive index of silica glass for infrared wavelengths by IR spectroscopy. Journal of Non-Crystalline Solids. 1998;223(1-2):158-163;Available from: https://doi.org/10.1016/s0022-3093(97)00438-9.
28. Vieweg M, Gissibl T, Pricking S, Kuhlmey BT, Wu DC, Eggleton BJ, Giessen H. Ultrafast nonlinear optofluidics in selectively liquid-filled photonic crystal fibers. Optics Express. 2010;18(24):25232-25240;Available from: https://doi.org/10.1364/OE.18.025232.
29. Agrawal GP. Nonlinear fiber optics (5th edition). Elsevier, Amsterdam. ISBN: 978-0-12-397023-7. 2013;Available from: https://doi.org/10.1016/C2011-0-00045-5.
30. HV Le, VT Hoang, G Stępniewski, TL Canh, NVT Minh, R Kasztelanic, M Klimczak, J Pniewski, KX Dinh, AM Heidt, R Buczyński. Low pump power coherent supercontinuum generation in heavy metal oxide solid-core photonic crystal fibers infiltrated with carbon tetrachloride covering 930-2500 nm. Optics Express. 2021;29(24):39586−39600;Available from: https://doi.org/10.1364/OE.443666.
31. Dudley JM, Taylor JR. Supercontinuum generation in optical fibers. Cambridge University Press. ISBN: 9780511750465. 2010;Available from: https://doi.org/10.1017/CBO9780511750465.
32. Meister J, Franzen R, Eyrich G, Bongartz J, Gutknecht N, Hering P. First clinical application of a liquid-corelight guide connected to an Er: YAG laser for oral treatment of leukoplakia. Laser in Medical Science. 2010;25(5):669-673;Available from: https://doi.org/10.1007/s10103-010-0782-0.
33. Tian L, Wei L, Guoying F. Numerical simulation of supercontinuum generation in liquid-filled photonic crystal fibers with a normal flat dispersion profile. Optics Communications. 2015;334:196−202;Available from: https://doi.org/10.1016/j.optcom.2014.07.080.